RESEARCH ARTICLE   OPEN ACCESS

Evaluation of Potential Use of the Dimensionless Temperature as a New Drought Index

Safa'a A. Ayyash *, Ayman A. Suleiman**
(Department of Land, Water and Environment. The University of Jordan, Jordan.)
** (Department of Land, Water and Environment. The University of Jordan, Jordan.)
Correspondng Author : Safa'a A. Ayyash

ABSTRACT
In this study, the use of the dimensionless temperature (ΔT) as a new agricultural drought index was investigated. A pilot study of one hectare planted to durum wheat seedlings of (Um Qais) variety was carried out in the Jordan Valley. The crop was planted on 2nd January and harvested on 1st June during the 2018 growing season. To mimic drought, irrigation of wheat was stopped at the beginning of flowering stage and continued until harvest. Remotely sensed canopy temperature was obtained from four Landsat-8 images during the growing season and converted to aerodynamic surface temperature using ALARM. The soil water content, leaf area index and plant height were measured in the field. Low values of ΔT indicated that sufficient amount of water was stored in the soil while high values of ΔT, indicated limited water content availability in the soil. ΔT was compared with Soil Water Deficit Index (SWDI), the results of the comparison between ΔT and SWDI showed a good agreement between the two indices.
Keywords - Dimensionless Temperature (ΔT); Drought; Soil Water Deficit Index (SWDI); Soil Water Content

I. INTRODUCTION

A drought is a natural disaster results from lack of precipitation over a time period. Usually, droughts cause a negative impact on water resources, crops production, environment, industry, natural ecosystems, households, hydro-power generation, recreation [1, 2, 3, 4]. Drought occurrence relays on many factors some of which are increasing temperatures, frequent winds of high speeds, low relative humidity, timing and characteristics of rain (e.g., frequency, intensity, and duration, the Eurasian atmospheric circulation patterns, and the El Niño effect [3, 5].

The common features of droughts in the majority of Mediterranean countries are: severe hydrological deficits ; drought - prone countries; the generalized response to drought hazard is a reactive approach using emergency actions instead a pro-active approach based on prevision and prevention tools; finally a limited exchange of experiences gained during severe droughts [6]. There is a general increase in the frequency, severity and duration of droughts in the recent years over many countries in the Mediterranean region [7and 8]. Droughts in Jordan in general move position with time from southern desert parts to northern desert parts and from the eastern desert parts to highlands and Jordan Rift Valley at the west. Jordan is confronting spatial and temporal variations in seasonal rainfall. More than 80 % of the country's area is arid usually, droughts in Jordan happen during January, February and March [9, 10].

Monitoring of droughts is very important to decrease the impact of such a damaging environmental phenomenon; especially in arid and semiarid regions. A drought can decrease plant production when a crop does not receive adequate rainfall or irrigation [11, 12]. A major challenge of detecting drought is finding reasonable methods that would help in determining the beginning, end and severity of droughts [13].

Drought indices are used to monitor and assess drought aimed at understanding drought intensity, duration, frequency and spatial extent. Four types of drought indices are available these are: meteorological drought which is defined by climatic variables; agricultural drought and is characterized by a shortage of available water for plant growth; hydrological drought, which is related to a period with inadequate surface and subsurface water resources to supply established water uses, and the socio-economic drought occurs when the demand for a commercial good exceeds supply as a result of weather-related event [14, 15]. These different drought indices are highly dependent on each other. Primarily meteorological drought indices are Standardized Precipitation Index, SPI which is the mostly used drought indices because of its simplsity to calculate and its reliability [1, 11, 16]. Standardized Precipitation Effectiveness Index, SPEI, and Palmer Drought Severity Index (PDSI), While Soil Wetness Deficit Index, (SWDI) and Soil Moisture Index (SMI) are used to represent agricultural droughts. Surface Water Supply Index,

(SWSI) and Effective Drought Index (EDI) are considered hydrological drought indices.

[17] developed the dimensionless temperature (ΔT), which is determined only in terms of the air temperature (Ta), aerodynamic surface temperature (Ti), which is widely used because it is readily available from satellites with thermal bands such as Landsat-8. Drought can affect the surface water balance via changing the surface sensible and latent heat fluxes. ΔT is simple to determine in the field and may to characterize the state of vegetated surfaces. Also, dimensionless temperature is useful because measured soil water for effective root zone is not needed for ΔT. Ability of this measure to indicate drought was tested in the present study. Subsequently, the specific objective of this study was to evaluating the potential use of the dimensionless temperature to predict drought.

II. MATERIALS AND METHODS

2.1 Study area

The experiment was carried out at the University of Jordan Agricultural Research Station (ARSUJ) in the Central Jordan Valley at 32° 10′ N latitude and 35° 37′ E longitude with an elevation of 230 meters below the sea level. The Jordan Valley has a warm climate in winter and a hot summer. The yearly average maximum and minimum temperatures are 30.9 and 18.5°C, respectively [18, 19].

2.2 Weather data

Ground weather data were collected from Deir Alla weather station that include air temperature, wind speed and net solar radiation at the time of satellite overpass are required weather parameters. During 2018 season, the mean monthly weather data are shown in (Table 1). During the growing season, the maximum temperatures reached to 45.2 °C in May while the minimum temperature was 7 °C in January. The highest mean net solar radiation (R_n) value was 250.78 W/m^2 in May while the lowest value was 89.88 W/m^2 in January. The maximum relative humidity (RH) was 92.10 in April while the minimum relative humidity was 11.05 in May. Average wind speed ranged from 2.00 to 2.37 m/s.

Table 1: Mean monthly weather data in Deir Alla station.

Month	Max of Temp	Min of Temp	Avg. of R_n W/m^2	Avg. of RH	Min of RH	Max of RH	Avg. of wind speed m/s
Jan	23.3	7.00	89.88	67.86	29.68	91.83	2.06
Feb	26.00	9.60	128.67	62.14	27.30	90.93	2.00
Mar	34.60	12.20	205.81	52.48	15.92	86.62	2.12
Apr	39.00	13.40	240.75	52.21	11.78	92.10	2.09
May	45.20	18.30	250.78	44.00	11.05	83.59	2.37

2.3 Wheat experiment

One hectare was planted to durum wheat of (Um Qais) variety. The crop was planted on 2nd Jan and harvested on 1st june. The wheat was drip irrigated with 0.25 m dripline spacing and a 0.4 m emitter spacing with an average discharge of 4 l/h. Soil samples were collected from four soil layers0-20, 20-40, 40-60, and 60-80 cm to determine some soil properties. The Pipette Method [20] was used to determine the texture of the soil in the study area. The Core Method was used to determine bulk density (Bd) as described by [21]. Field capacity (Θ_{FC}) and permanent wilting point (Θ_{pwp}) were determined using ceramic plate method as described by [22]. The soil texture analysis showed that the soil in the study area is loamy sand at the first two layers and sandy loam for the next two layers, the soil Bd was 1.62 g/cm^3, the Θ_{pwp} varied between 0.08 cm^3/cm^3 at the upper layers to 0.11 cm^3/cm^3 in the lower part of the soil profile and the Θ_{FC} ranged from 0.17 to 0.21 cm^3/cm^3.

The measurements of the volumetric soil water content at the four soil layers were taken using Time Domain Reflectometer (TDR). Twenty access tubes of 1m height were installed in the wheat field five of them in the center of each the four Landsat-8 pixels within the study area. Four full wheat covered Landsat-8 pixels of 30 m were found in the study area. Letters were assigned to each pixel to illustrate their alignment in the study (Fig. 1). The measurements of the volumetric soil water content with the TDR probe at depths of 0–20, 20–40, 40–60, and 60–80 cm were conducted once a day in the morning from 12th Mar, 2018 to 20th Apr, 2018 and at the landsat-8 images acquisition dates in the morning of the overpass day and in the morning after 24 hr.
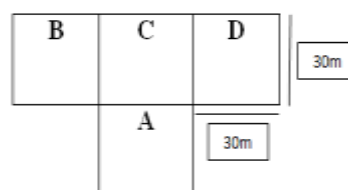

Figure 1: Pixels Alignment in the field.

The leaf area index (LAI) was measured on the four landsat-8 image dates by using a portable Decagon's LP-80 ceptometer (AccuPAR LP-80) device inside the wheat field with four full covered pixels and plant height was recorded. Each LAI measurement is a result from the mean of five readings per pixel.

2.4 Satellite images downloading and processing

Four Landsat-8 images, which pass over an area every 16 days, were downloaded from USGS website [23]. Thermal band (band 10 in Landsat-8) was used for the computation of radiometric surface temperature. The images were taken on 12th Mar, 13th Apr, 15th May and 31st May, 2018. In the image processing, geometric and radiometric correction procedures was conducted to make Landsat-8 data comparable with in situ measurements.

To mimic drought irrigation of wheat was stopped at the beginning of flowering stage and continued until harvest, because in flowering stage wheat is most sensitive to drought [5, 24].

2.5 Dimensionless Temperature (ΔT)

[25] developed the Analytical Land Atmosphere Radiometer Model (ALARM) to convert the radiometric surface temperature (T_r) to a well-defined aerodynamic surface temperature (T_i) by correcting for vegetation temperature profile and considering LAI, canopy height, fractional cover, leaf angle distribution, and zenith sensor view angle estimate. Radiometric surface temperature is widely used because it is readily available from satellites with thermal bands. Ti is the temperature required by the surface to give the correct sensible heat flux if the canopy were isothermal [25, 26]. The study area was cloud-free during the four Landsat-8 images taken. The Landsat-8 multispectral bands resolution is 30 m while the thermal band resolution is 100 m which is resampled to 30 m to match the multispectral bands.

[17] defined a dimensionless temperature (ΔT) as follows:

$$\Delta T = (T_i - T_a)/ (T_{max} - T_a) \qquad (1)$$

where; T_i is the aerodynamic surface temperature, T_a is the air temperature and T_{max} is maximum surface temperature that would occur if all the net radiation (R_n) was converted to sensible heat flux and no evaporation occurred.

To calculate T_{max}, the sensible heat is assumed equal R_n. The sensible (H, W m^{-2}) heat flux into the atmosphere [27] can be calculated from:

$$H = \frac{(T_s - T_a) k u^* \rho c_p}{\left[\ln\left\{ \frac{z_a - d_o}{z_{oh}} \right\} - \psi \left\{ \frac{z_a - d_o}{L} \right\} \right]} \qquad (2)$$

Where T_s (^oC) is the surface temperature, T_a (^oC) is the air temperature at a height z_a (m) in the surface sublayer, k (where k=0.4) is von-Karman's constant, u* (ms^{-1}) is the friction velocity, ρ(kg m^{-3}) is the density of the air, cp (J kg-$^{10}C^{-1}$) is the specific heat at constant pressure, z_{oh} (m) is the scalar roughness length for sensible heat transfer, and do (m) was the displacement height. Atmospheric stability, which affects the efficiency of turbulent transport, was included through the variable ψ, which is a function of the stability or buoyancy parameter (z_a - d_o)/L, where L (m) is the Obukhov length [27].

ΔT equals or less than one and can be negative when the air T_a is greater than T_i, such as for advection condition. To calculate ΔT, ground based and remotely sensed data are needed. Calculation steps showed in (Fig. 2). The index was compared using agricultural index SWDI [28]. SWDI was calculated using root zone soil water content.
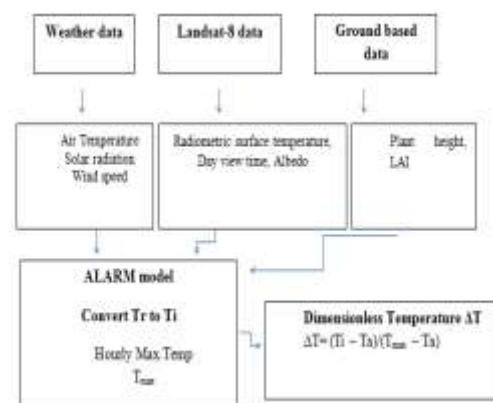

Figure 2: Calculation steps of Dimensionless Temperature (ΔT).

2.6. Soil Water Deficit Index SWDI

SWDI was developed by [28] to use soil water content for drought monitoring, and it is calculated as follows:

$$SWDI = (\Theta - \Theta_{FC})/\Theta_{AWC} \qquad (3)$$

where; Θ is the volumetric soil water content; Θ_{FC} is the field capacity; Θ_{PWP} is the permanent wilting point and Θ_{AWC} is available water content, which is the difference between Θ_{FC} and Θ_{PWP},. SWDI is a fractional magnitude. When the SWDI is positive, the soils have excess water; when it equals zero, the soil is at the field capacity of water content (i.e., no water deficit). Negative values indicate a soil drought, and the water deficit is absolute (wilting point) when the SWDI reaches =< -1 at this point, the soil water content is below the lower limit of available water for plants. Table 2 shows SWDI severity categories. The SWDI was daily determined for the soil root zone and compared with the ΔT on the image dates.

Table 2: SWDI severity categories

SWDI value	Drought level
SWDI > 0	No drought
0 > SWDI >-0.2	Mild
-0.2 > SWDI >-0.5	Moderate
-0.5 > SWDI >-1.00	Severe
-1> SWDI	Extreme
Source: Fernández et al., (2015)	

III. RESULTS AND DISCUSSION

3.1 Soil water content measurements

Sharp decline in soil water content for the surface layer (0-20 cm) was observed for the different pixels due to its contact with the atmosphere and soil evaporation and water uptake that is mostly in the surface layer especially under drip irrigation. The (20-40) cm and (40-60) cm layers had slight differences in soil water content while the last soil layer was the least variable in soil water content. Also, the soil of the study area had high sand percentage and relatively low water holding capacity which leads to faster change in the soil water content in the soil.

3.1 Leaf Area Index (LAI)

Fig. 3 shows LAI at the image dates for the four pixels. LAI was highest in March, intermediate in April and lowest in May. This because on 12th Mar the wheat was at the flowering stage, but on 15th May and 31st May the wheat was at the grain filing stage.
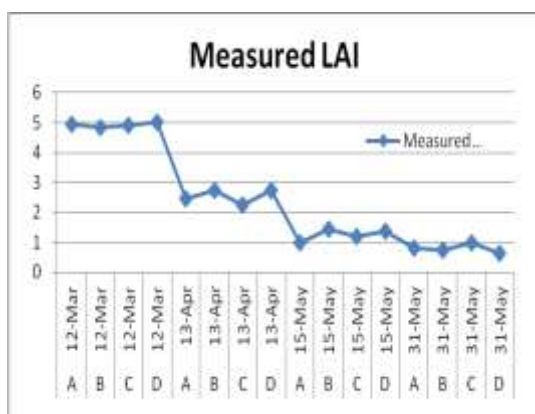

Figure 3: Measured LAI on the image dates at the four pixels

3.3 Dimensionless Temperature

Fig. 4 shows the aerodynamic surface temperature, air temperature and maximum temperature values at different Landsat-8 images. Aerodynamic surface temperature values were higher than air temperature values for all pixels. The differences between them increased when water stress is increasing because of limited water in the

soil, causing the surface to become warmer with time. Although, the maximum temperature and the aerodynamic surface temperature had the same trend, the maximum temperature was higher than the aerodynamic surface temperature throughout water stress part of the experiment.
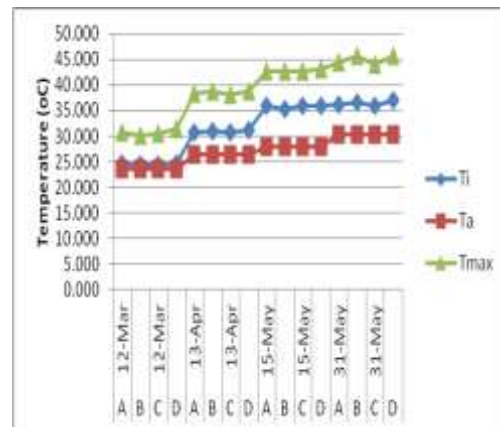

Figure 4: T_a, T_i and T_{max} at the study area.

The minimum ΔT value for the different pixels was 0.14 in March, while the maximum was 0.55 in May (Fig. 5). ΔT on 12th Mar was low because the study area was irrigated. ΔT values were higher for the other dates because the wheat was under water stress because of irrigation stopped at the beginning of flowering stage. Low values of ΔT indicated that sufficient amount of water was stored in the soil, while high values of ΔT indicated limited water content availability in the soil profile. ΔT on the 31st May was low due to dust or other unseen variable affect the image from landsat-8.
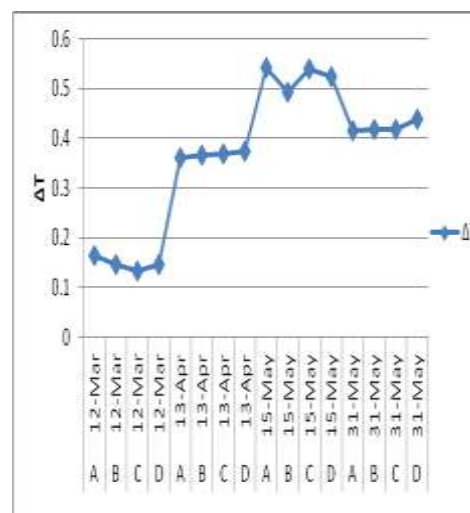

Figure 5: ΔT calculated for different pixels in the study area on the four landsat-8 images.

3.4 Comparison with SWDI

SWDI decreased at all pixels over time from 12th Mar to 20th Apr (Fig. 6). Also, it showed

that a decline in SWDI is a good indicator for a drought happening over the time. On 12th Mar, 2018, the SWDI ranged from -0.16 to -0.05 which is under mild drought category as mentioned in [28]. SWDI for image 13th Apr, 2018 was in the moderate drought category range from -0.49 to -0.44. On 15th May image the SWDI ranged from -0.96 to -0.82, which is severe drought indicated that soil water content far below field capacity. Finally on 31st May, the range of SWDI from -1.20 to -1.02 was under extreme category.
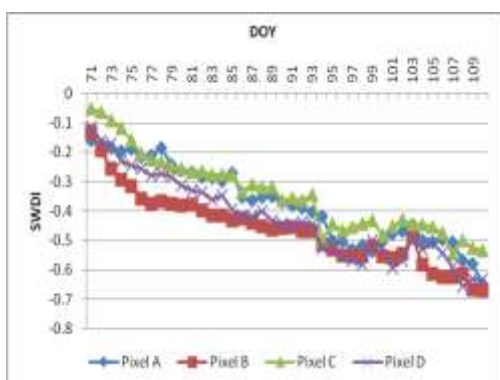

Figure 6: The SWDI derived from observed soil water content at pixel A, B, C, D during the growing season (DOY 71–109), 2018.

When SWDI was highest on 12th Mar, the ΔT had its lowest values which may be attributed to high available soil water (Fig. 7). Also, when the SWDI values decreased the ΔT values increased. This indicated that ΔT is capable of monitoring drought successfully.
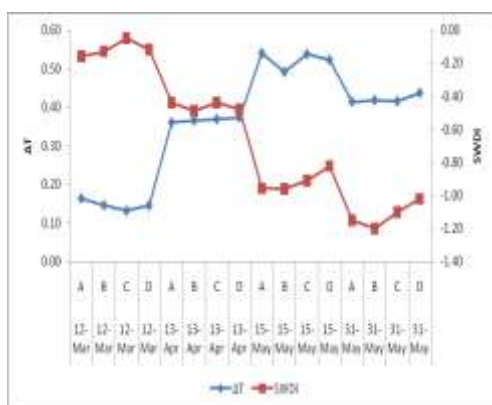

Figure 7: SWDI and ΔT at the study area during four image dates.

The results of the comparison also showed a good agreement between two indices (Fig. 8). The coefficient of determination (R^2) between ΔT and SWDI was 0.717.The ΔT is directly related to actual evapotranspiration [17] while SWDI is dependent on the soil water content which influences the actual evapotranspiration greatly.
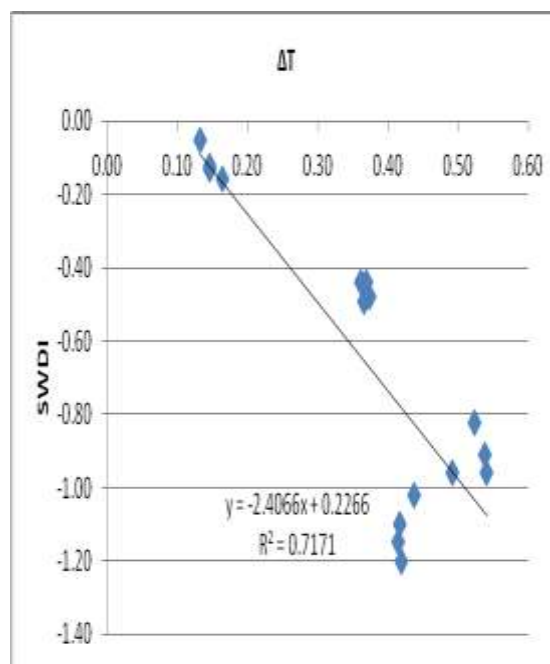

Figure 8: Correlation between ΔT and SWDI.

IV.   CONCLUSIONS

In this study, the dimensionless temperature (ΔT) was tested as a new agricultural drought index. One hectare planted to durum wheat seedlings of (Um Qais) variety in the Jordan Valley. Low values of ΔT indicated that sufficient amount of water was stored in the soil, while high values of ΔT, indicated limited water content availability in the soil profile. These results indicated that ΔT is capable of identifying drought. The results of the comparison between ΔT and SWDI showed a good agreement between the two indices.

REFERENCES

[1]. I Livada, V. D. Assimakopoulos, Spatial and temporal analysis of drought in Greece using the Standardized Precipitation Index (SPI), Theor. Appl. Climatol., 89, 2007, 143-153.
[2]. P Dahal, N. S. Shrestha, M.L. Shrestha, N.Y. Krakauer, J. Panthi, S.M. Pradhanang, A. Jha, T. Lakhankar, Drought risk assessment in central Nepal: temporal and spatial analysis. Nat. Hazards., 80, 2016, 1913-1932.
[3]. S Benlin, Z. Xinyu, H. Yunchuan, Y. Yanyan, Drought characteristics of Henan province in 1961-2013 based on Standardized Precipitation Evapotranspiration Index. Geogr. Sci., 27(3), 2017, 311-325.
[4]. C Chen, W. Wu, H. Liu, Assessing the utility of meteorological drought indices in monitoring summer drought based on soil moisture in Chongqing, Theor. Appl. Climatol., 2017.
[5]. A Belal, H. El-Ramady, E. Mohamed,A. Saleh, Drought risk assessment using remote sensing and GIS techniques. Arab J Geosci., 7, 2014, 35-53.
[6]. G Rossi, An Integrated Approach to Drought Mitigation in Mediterranean Regions. Tools for

Safa'a A. Ayyash Journal of Engineering Research and Application
w.ijera.com
ISSN : 2248-9622 Vol. 9,Issue 5 (Series -V) May 2019, pp 21-26

drought mitigation in Mediterranean regions, Kluwer Academic Publishers, Netherlands, 2003, 3-18.

[7]. A Cancelliere, A. and G. Rossi, Droughts in Sicily and Comparison of Identified Droughts in Mediterranean Regions. Tools for drought mitigation in Mediterranean regions. Kluwer Academic Publishers, Netherlands, 2003, 103-122.

[8]. S Michaelides, T. Karacostasc , J. L. Sánchezd , A. Retalise , I. Pytharoulisc , V. Homarf , R. Romerof , P. Zanisc , C. Giannakopoulose , J. Bühlg , A. Ansmanng ,A. Merinod , P. Melcónd , K. Lagouvardose ,V. Kotronie , A. Bruggemana , J. I. López-Morenoh , C. Bertheti , E. Katragkouc , F. Tymviosa, D. G. Hadjimitsis, R. M. A. Nisantzib, Atmosheric Research, 208, 2018, 4-44.

[9]. M Al-Qinna, N. Hammouri, M. Obeidat, F. Ahmad, Drought analysis in Jordan under current and future climates. Climatic Change., 106,2011, 421-440

[10]. M Shatanawi, Y. Al-Zu'bi, O. Al-Jayoussi, Irrigation management dynamics in the Jordan Valley under drought conditions. Tools for drought mitigation in Mediterranean regions, Kluwer Academic Publishers, Netherlands, 2003, 243-258.

[11]. S Liu, W. Kang, T. Wang, Drought variability in Inner Mongolia of northern China during 1960–2013 based on standardized precipitation evapotranspiration index. Environ. Earth Sci., 2016, 75:145

[12]. M Tan, F. Liao, L. Hou, J. Wang, L. Wei, H. Jian, X. Xu, J. Li, L. LiuEuphytica, Genome-wide association analysis of seed germination percentage and germination index in Brassica napus L. under salt and drought stresses. Euphytica. 2017, 213-240.

[13]. A Zarei, M. Moghimi, M. Mahmoudi, Parametric and Non-Parametric Trend of Drought in Arid and Semi-Arid Regions Using RDI Index. Water Resour. Manage., 30, 2016, 5479-5500.

[14]. L Vasiliades, A. Loukas, N.A. Liberis, Water Balance Derived Drought Index for Pinios River Basin, Greece Resour. Manage., 25, 2011, 1087-1101.

[15]. N Bandyopadhyay, K. Saha, A comparative analysis of four drought indices using geospatial data in Gujarat, India, Arab J Geosci., 9, 2016, 341

[16]. J Yoo, H. Kwon, J. Lee, T. Kim, Influence of Evapotranspiration on Future Drought Risk Using Bivariate Drought Frequency Curves, KSCE Journal of Civil Engineering, 20(5), 2016, 2059-2069.

[17]. A A Suleiman, R. D. Crago, Hourly and daytime evapotranspiration using radiometric surface temperatures. Agronomy J. 96 (2), 2004, 384–390

[18]. A Suleiman, J. Al-Bakri, M. Duqqah, M. and R. Crago, Intercomparison of evapotranspiration estimates at the different ecological zones in Jordan. American Meteorological Society, 2008, 903-919.

[19]. R Al-Qerem, Assessing and Modeling Tomato Yield and Water Saving Under Water Deficit in Jordan Valley. M.Sc. Thesis, University of Jordan, Amman, Jordan, 2010.

[20]. G.W. Gee, J.W.B. Bauder, Particle size distribution, In: Klute, A. (ED.), Methods of Soil analysis, Part 1, (2nd ED.), Physical and Mineralogical Methods, (Agronomy Society of America and Soil Science Society of America, Madison, Wisconsin, 1986).

[21]. G R Blake, K.H. Hartge, Bulk density, In: Klute, A. (ED.), Methods of Soil Analysis, Part 1, (2nd ED.), Physical and Mineralogical Methods, (Agronomy Society of America and Soil Science Society of America, Madison, Wisconsin, 1986), 363-382.

[22]. D K Cassel, D.R. Nielsen, Field capacity and available water capacity. In: Klute, A. (ED.), Methods of Soil Analysis, Part I, (2nd ED.), Physical and Mineralogical Methods. (Agronomy Society of America and Soil Science Society of America, Madison, Wisconsin, 1986), 901–926.

[23]. http://glovis.usgs.gov/

[24]. B Narasimhan, R. Srinivasan, development and evaluation of soil moisture deficit index (SMDI) and evaporation deficit index (ETDI) for agricultural drought index, Agriculture and Forest Metrology, 133, 2005, 69-88.

[25]. A A Suleiman, R.D. Crago, Analytical land atmosphere radiometer model. Appl. Meteorol. J., 41 (2), 2002, 177–187.

[26]. A A Suleiman, R.D. Crago, Analytical land atmosphere radiometer model (ALARM) applied to a dense canopy. Agric. Forest Meteorol,. 112 (3–4), 2002. 151–159.

[27]. W Brutsaert, Evaporation into the atmosphere (edited by D. Reidel, Dordrecht, Netherlands: Springer, 1982).

[28]. J Martínez-Fernández, A. González-Zamora, N. Sánchez, A. Gumuzzio, Soil water based index as a suitable agricultural drought indicator, Journal of Hydrology, 522, 2015, 265–273.